



## Dual overcharge protection and solid electrolyte interphase-improving action in Li-ion cells containing a *bis*-annulated dialkoxyarene electrolyte additive



Jingjing Zhang<sup>a,b</sup>, Ilya A. Shkrob<sup>a,b</sup>, Rajeev S. Assary<sup>a,c</sup>, Shuo Zhang<sup>a,b</sup>, Bin Hu<sup>b</sup>, Chen Liao<sup>a,b</sup>, Zhengcheng Zhang<sup>a,b</sup>, Lu Zhang<sup>a,b,\*</sup>

<sup>a</sup> Joint Center for Energy Storage Research, Argonne National Laboratory, 9700 South Cass Avenue, Lemont, IL 60439, USA

<sup>b</sup> Chemical Sciences and Engineering Division, Argonne National Laboratory, 9700 South Cass Avenue, Lemont, IL 60439, USA

<sup>c</sup> Materials Science Division, Argonne National Laboratory, 9700 South Cass Avenue, Lemont, IL 60439, USA

### HIGHLIGHTS

- A stable redox shuttle molecule, BODMA, has been developed and evaluated.
- BODMA is electrochemically reversible at 4.0 V vs Li/Li<sup>+</sup>.
- BODMA provided over 120 cycles of overcharge protection at 100% abuse ratio at C/5 rate.
- BODMA decreases the impedance of the Li-ion cells, demonstrating dual functionality.

### ARTICLE INFO

#### Keywords:

Redox shuttle  
Electrolyte additive  
Overcharge protection  
High stability  
Low impedance  
Lithium-ion batteries

### ABSTRACT

1,4-Dialkoxybenzene additives are commonly used as redox active shuttles in lithium-ion batteries in order to prevent runaway oxidation of electrolyte when overcharge conditions set in. During this action the shuttle molecule goes through a futile cycle, becoming oxidized at the cathode and reduced at the anode. Minimizing parasitic reactions in all states of charge is paramount for sustained protective action. Here we demonstrate that recently developed *bis*-annulated 9,10-*bis*(2-methoxyethoxy)-1,2,3,4,5,6,7,8-octahydro-1,4:5,8-dimethano-anthracene shuttle molecule (that yields exceptionally stable radical cations) survives over 120 cycles of overcharge abuse with 100% overcharge ratio at C/5 rate. Equally remarkably, in the presence of this additive the cell impedance becomes significantly lower compared to the control cells without the additive; this decrease is observed during the formation, normal cycling, and even under overcharge conditions. This unusual dual action has not been observed in other redox shuttle systems, and it presents considerable practical interest.

Lithium-ion batteries (LIBs) are ubiquitous in our world [1]. Overcharge protection of these commercially successful batteries remains a concern due to extensive component damage, overheating, and even explosions that occur when overcharge conditions set in [2–6]. Under these conditions, the redundant electric energy accumulates at the electrode surface sharply increasing the voltage and causing exothermic reactions due to electrolyte oxidation [1,7,8]. Electrolyte additives, such as redox shuttles, offer a cost-efficient option for overcharge protection [3,9,10]. Such molecules (S) exhibit nearly perfect electrochemical reversibility at the redox potentials that are ~0.3–0.5 V higher than the end-of-charge potential of the cathode [11]. When the cell enters the overcharge state, the molecules get oxidized by the

external charging current to form radical cations S<sup>•+</sup> near the electrode surface; this radical cation diffuses to the anode where it discharges back to S, completing the cycle. This shuttling operation can continuously carry the electric current during overcharging, thereby protecting the cell [12–14]. Generally, the number of overcharge cycles is limited by parasitic reactions of S<sup>•+</sup> that occur both in the bulk and near the two electrodes. As the redox shuttle molecule becomes consumed in these reactions, overcharge abuse sets in and the cell fails. Thus, minimization of parasitic reactions is paramount for sustained protective action. Unless these reactions are suppressed, only the increased concentration of the shuttle molecules can extend the protective action, as it takes longer time to consume them entirely; however,

\* Corresponding author. Joint Center for Energy Storage Research, Argonne National Laboratory, 9700 South Cass Avenue, Lemont, IL 60439, USA, Chemical Sciences and Engineering Division, Argonne National Laboratory, 9700 South Cass Avenue, Lemont, IL 60439, USA.

E-mail address: [luzhang@anl.gov](mailto:luzhang@anl.gov) (L. Zhang).

<https://doi.org/10.1016/j.jpowsour.2017.12.059>

Received 1 September 2017; Received in revised form 5 December 2017; Accepted 19 December 2017  
0378-7753/© 2017 Elsevier B.V. All rights reserved.

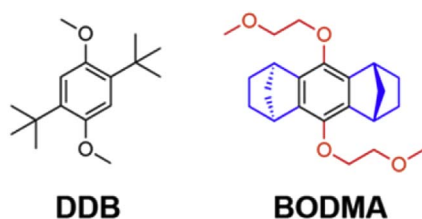


Fig. 1. Structures and acronyms for the 1,4-dialkoxybenzene derivatives discussed in this paper.

increasing this concentration may not be advisable as the reaction products can interfere with the normal operation of the cell by modification of solid-electrolyte interphases (SEIs) that shield the electrodes from the electrolyte. These reaction products can form deposits that block  $\text{Li}^+$  ion conduction through the SEI layers increasing the cell impedance [11,15], so even when the overcharge conditions cease to exist and the cell operates normally, the cell performance (in the normal operation regime) is still degraded. In this communication, we report a redox shuttle molecule that does not cause this increase in the impedance; actually, it lowers this impedance after normal and/or overcharge abuse cycling.

This molecule is 9,10-bis(2-methoxyethoxy)-1,2,3,4,5,6,7,8-octahydro-1,4:5,8-dimethanoanthracene (BODMA) shown in Fig. 1. It belongs to the family of 1,4-dialkoxyarene derivatives that have long been considered for use as redox shuttles in LIBs [16]. In particular, Dahn and co-workers popularized the use of 2,5-di-*tert*-butyl-1,4-dimethoxybenzene (DDB, also shown in Fig. 1) [17]. However, parasitic reactions of the radical cation of DDB (in particular, the loss of *tert*-butyl group and *O*-dealkylation) still occur limiting the cycling life [18,19], while the relatively low solubility of DDB in carbonate electrolytes impedes one's ability to extend the protective action through concentration increase (see above).

A striking feature of BODMA is the excellent stability of  $\text{BODMA}^{\bullet+}$  in the common electrolytes [20]. In this species, the arene ring is fully substituted, precluding radical addition reactions, and slow *O*-dealkylation is the only remaining reaction of this radical cation. A favourable property of BODMA (conducive to its use as a redox shuttle in LIBs) is its excellent solubility in the common carbonate electrolytes ( $\sim 0.2$  M vs.  $\sim 80$  mM for DDB).

As indicated by cyclic voltammetry (Fig. 2, see ESI for all experimental details), electrochemical oxidation of BODMA in Gen2 electrolyte is fully reversible. (Gen2 is the commercial standard for LIBs, which is a 3:7 w/w liquid mixture of ethylene carbonate and ethyl methyl carbonate containing 1.2 M  $\text{LiPF}_6$ ). Oxidation at 4.0 V vs.  $\text{Li}/\text{Li}^+$  implies that BODMA can protect lithium ferrous phosphate ( $\text{LiFePO}_4$ ) cathode, which has an end-of-charge potential of  $\sim 3.5$  V vs.  $\text{Li}/\text{Li}^+$ . Fig. 3 shows the voltage profile of the overcharge test using a 2032-coin cell with the mesocarbon microbead (MCMB) graphitic anode and  $\text{LiFePO}_4$  cathode;

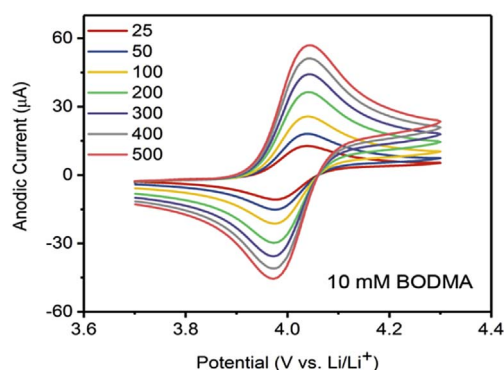


Fig. 2. Cyclic voltammograms for 10 mM BODMA in Gen 2 electrolyte at various scan rates (mV/s) obtained using Pt/Li electrodes at 25 °C.

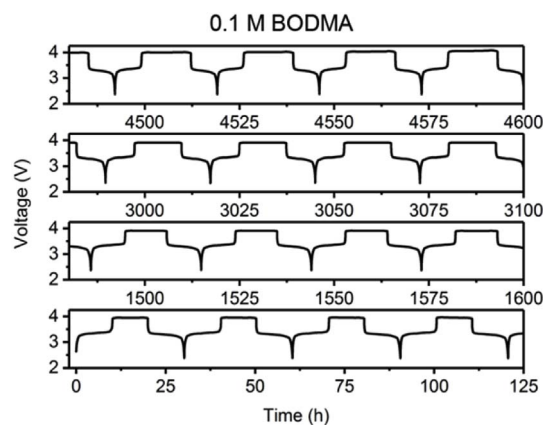


Fig. 3. Voltage profiles of overcharge tests using the MCMB/ $\text{LiFePO}_4$  coin cell containing 0.1 M BODMA in Gen 2 electrolyte over 4600 h. The charging rate is  $C/10$  and the overcharge ratio is 100%.

this cell contained 0.1 M BODMA in Gen2. After two formation cycles, the cell was charged for 20 h at  $C/10$  rate to achieve 100% overcharge (at which the overcharge and normal charge capacities become equal). As shown in Fig. 3, the first charging plateau occurred at  $\sim 3.4$  V, indicating the normal charging process of the  $\text{LiFePO}_4$  cathode. Once the full cell capacity was reached, the cell voltage climbed to 3.9 V, at which the BODMA shuttle was activated. As a result, a flat plateau (corresponding to oxidation and reduction of BODMA) was observed for the next 10 h. The cell was then discharged to quantify the discharge capacity. This cycling was continued until the shuttling action failed. Fig. 3 indicates that even under these extremely abusive conditions, BODMA protected the cell for 4600 + h. At the end of this test, the cell still provided 70% of the initial discharge capacity. The discharge capacity gradually faded as the test progressed (Fig. S2), which is common in such tests due to irreversible Li loss in the cathode caused by deleterious reactions occurring when the cell potential exceeds the threshold of normal charge of the cathode but is still lower than the oxidation potential of the redox shuttle [14].

A higher concentration of this redox shuttle additive can sustain overcharge abuse for a higher current. This is illustrated in Fig. 4: for 0.2 M BODMA electrolyte, a coin cell cycled at  $C/5$  rate was able to provide efficient overcharge protection for 1820 h, which is equivalent to 120 + overcharge cycles.

A frequent concern with the redox shuttle electrolyte additives is their interference with the normal operation of the cell. As shown in Fig. S3 in ESI, under  $C/3$  rate cycling, the cycling performance of the cells containing 0.2 M BODMA was similar to the control cells containing no BODMA. Actually, the overall performance for the BODMA-containing cell was slightly better than for the control cells with a higher capacity after 200 cycles, which is uncommon since the redox shuttles in the electrolyte typically increase cell polarization. Following this unexpected result, differential capacity and impedance measurements at different stages of cell cycling were carried out. No direct participation of BODMA in the SEI formation was apparent in the differential capacity profiles shown in Fig. S4 in ESI, suggesting that this molecule is neither oxidized nor reduced on the energized electrodes in preference to other electrolyte components. Despite this lack of direct redox chemistry, the presence of BODMA had significant effect on the cell impedance. In Fig. 5 we compare the impedances of the cells containing BODMA with the control cells without BODMA. After the formation cycles (Fig. 5a), the control cell demonstrated the greatest high frequency arc width among the three cells shown in Fig. 5a. As the concentration of BODMA increased, this width progressively decreased (Fig. 5a). The same trend was observed in the cells examined after 10 normal cycles (Fig. 5b). More strikingly, this decrease persisted when the 10 normal cycles were followed by 10 overcharge abuse cycles; the

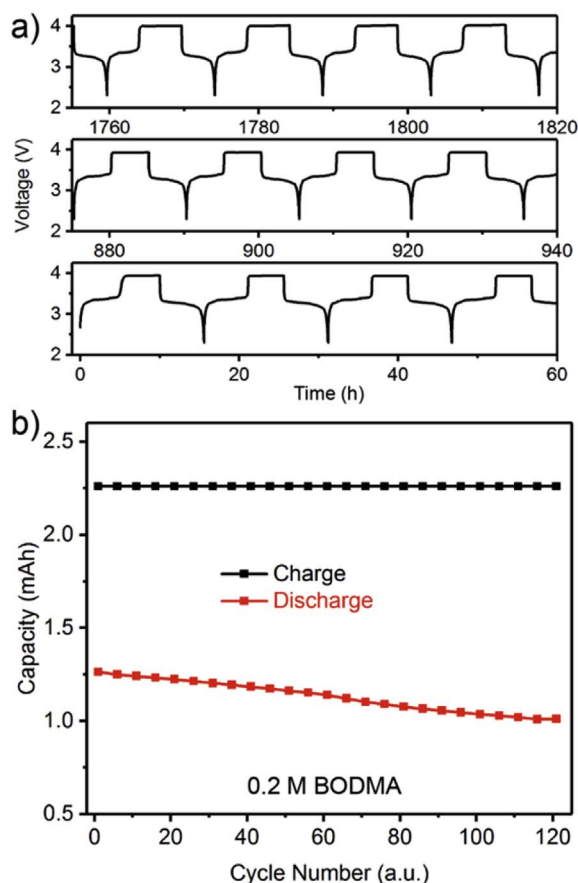


Fig. 4. Voltage profiles of overcharge abuse tests using the MCMB/LiFePO<sub>4</sub> coin cell containing 0.2 M BODMA in Gen 2 electrolyte during 1820 h of cycling. The charging rate is C/5 and the overcharge ratio is 100%. b) Capacity profiles of overcharge abuse.

impedance of the BODMA-containing cells was > 2 times lower compared to the control cells operated for 20 normal cycles (Fig. 5c). We conclude that BODMA not only provides efficient overcharge protection over a long period of time, but somehow improves Li<sup>+</sup> conduction through the SEI layers before and after overcharge conditions, contributing to the improved normal cycling performance. As shown in Fig. S5 in ESI, the decrease in the impedance due to BODMA presence in the electrolyte involves both of the electrodes, but the effect on the negative electrode is greater.

The protective action of BODMA can also be demonstrated in the scanning electron microscopy (SEM) images of the electrodes shown in Fig. 6. For MCMB electrodes, no obvious morphology changes were observed in the presence of 0.2 M BODMA (Fig. 6, panels a to d). On the cathode side, however, addition of BODMA led to better morphology of LiFePO<sub>4</sub> particles (Fig. 6g) compared to the control cell (Fig. 6e), and this effect was apparent already after two formation cycles. This difference became still greater after 10 normal cycles (Fig. 6f and h). In the control cell, the spaces between the cathode particles became filled with deposits; these deposits were not observed in the BODMA-containing cells.

It is known that solid SEI-like deposits on LiFePO<sub>4</sub> (which normally operates at voltages that are too low for electrolyte oxidation) are formed through the reactions of hydrolytically generated Brønsted and Lewis acids (such as HF and PF<sub>5</sub>) that cause LiF and Li<sub>x</sub>PO<sub>y</sub>F<sub>z</sub> formation [21], iron dissolution [22–24], and cationic polymerization of the solvent molecules [25,26]. Such polymer species are also formed on the anode via anionic polymerization [27,28]. Less sterically protected 1,4-dialkoxybenzenes can be involved in such reactions (e.g., electrophilic addition in the arene ring), promoting the formation of deposits, whereas the sterically protected BODMA avoids these reactions. It is

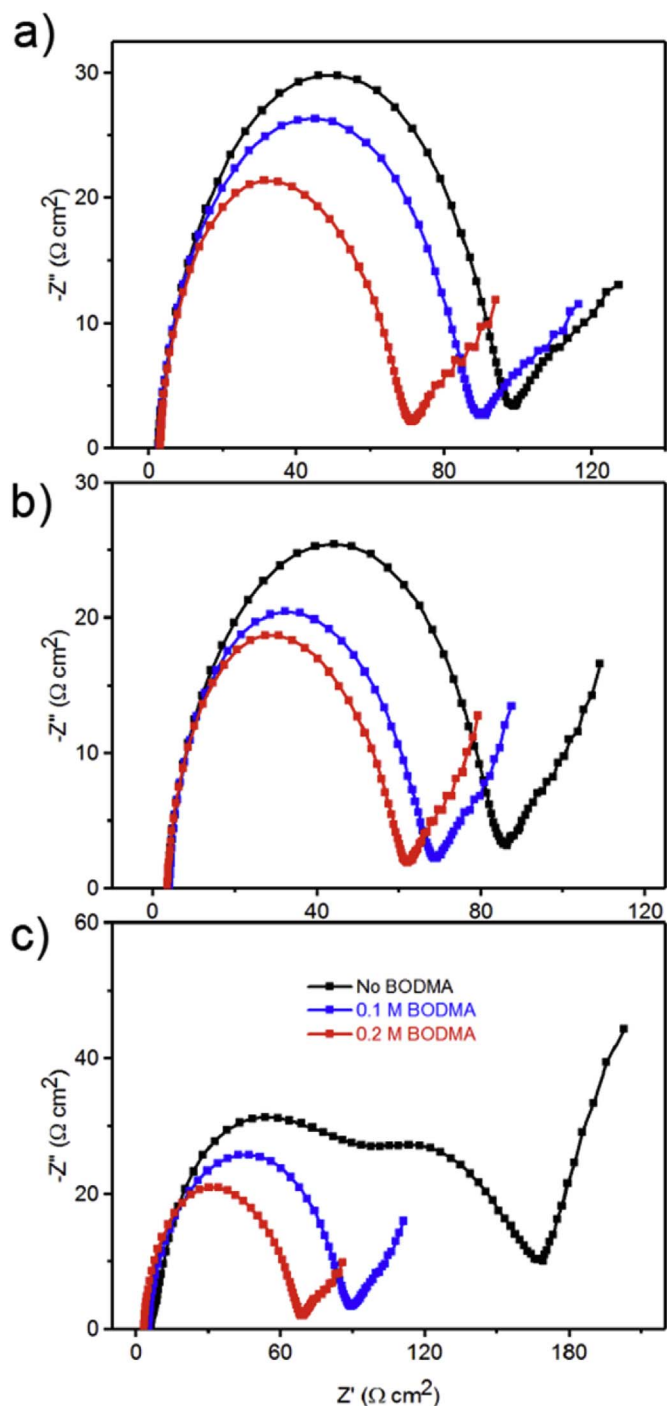
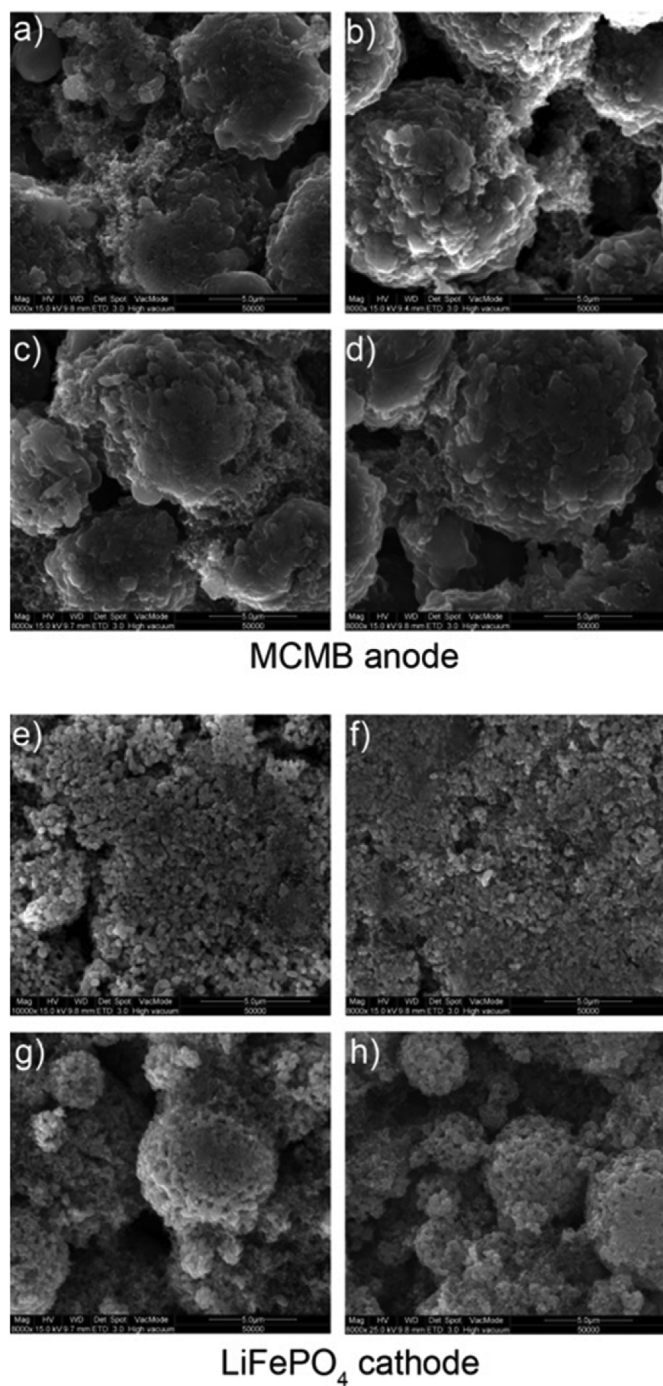


Fig. 5. Nyquist plots of a) MCMB/LiFePO<sub>4</sub> cells containing no BODMA, 0.1 M BODMA or 0.2 M BODMA in Gen 2 electrolyte after SEI formation at a rate of C/10; b) MCMB/LiFePO<sub>4</sub> cells containing no BODMA, 0.1 M BODMA or 0.2 M BODMA in Gen 2 electrolyte after 10 normal cycles at C/5; c) MCMB/LiFePO<sub>4</sub> cells containing no BODMA after another 10 normal cycles at C/5, 0.1 M BODMA or 0.2 M BODMA in Gen 2 electrolyte after 10 overcharge cycles at C/5 and 100% overcharge ratio.

more difficult to explain how BODMA-containing electrolytes decrease the impedance compared to the control cells. The effect can only be indirect, as BODMA is neither reduced nor oxidized during the formation and normal cycles; apparently, it acts as an SEI-improving agent. Such agents can be indirectly involved in the reactions of (radical) anions generated by reduction of the carbonate electrolyte [28]. There has been a precedent for this action when anisole (methoxybenzene) was used as electrolyte additive; the benign action was traced to the



**Fig. 6.** Scanning electron microscopy images of the harvested MCMB anodes: a) Gen 2 electrolyte after the SEI formation at C/10; b) Gen 2 electrolyte after 10 normal cycles at C/5; c) 0.2 M BODMA in Gen 2 electrolyte after the SEI formation at C/10; d) 0.2 M BODMA in Gen 2 electrolyte after 10 overcharge cycles at C/5 and 100% overcharge ratio. Below: scanning electron microscopy images of the harvested LiFePO<sub>4</sub> cathodes: e) Gen 2 electrolyte after the SEI formation at C/10; f) Gen 2 electrolyte after 10 normal cycles at C/5; g) 0.2 M BODMA in Gen 2 electrolyte after the SEI formation at C/10; h) 0.2 M BODMA in Gen 2 electrolyte after 10 overcharge cycles at C/5 and 100% overcharge ratio.

formation of lithium methoxide in the SEI [29]. Analogous reactions may occur for BODMA. While more needs to be learned to elucidate the mechanistic underpinnings of BODMA action, our results make it clear that it has cell chemistry that is different from the one exhibited by less substituted 1,4-dialkoxyarene redox shuttle molecules.

## Conclusions

We assessed the performance of a highly soluble, superbly sterically protected 1,4-dialkoxyarene molecule, BODMA, as a potential redox shuttle for overcharge protection of LiFeO<sub>4</sub> cathodes in Li-ion batteries. Using 0.2 M BODMA in Gen 2 electrolyte, we demonstrated that a MCMB/LiFeO<sub>4</sub> cell can survive 120 + overcharge abuse cycles at C/5 rate and 100% overcharge ratio. Unexpectedly, the cells containing 0.1–0.2 M BODMA also demonstrated significantly lower impedance compared to the control cells containing no BODMA, and the fouling of the cathode surface was visibly reduced. We believe that this is the first incidence of overcharge protection *and* SEI-improving functionalities combined in a single molecule, which makes this electrolyte additive both unusual and practically interesting.

## Acknowledgements

This work was supported as part of the Joint Center for Energy Storage Research (JCESR), an Energy Innovation Hub funded by the U.S. Department of Energy, Office of Science, Basic Energy Sciences. The submitted manuscript has been created by UChicago Argonne, LLC, Operator of Argonne National Laboratory (“Argonne”). Argonne, a U.S. Department of Energy Office of Science laboratory, is operated under Contract no. DE-AC02-06CH11357.

## Appendix A. Supplementary data

Supplementary data related to this article can be found at <http://dx.doi.org/10.1016/j.jpowsour.2017.12.059>.

## References

- [1] T. Ohsaki, T. Kishi, T. Kuboki, N. Takami, N. Shimura, Y. Sato, M. Sekino, A. Satoh, *J. Power Sources* 146 (2005) 97–100.
- [2] P.G. Balakrishnan, R. Ramesh, T. Prem Kumar, *J. Power Sources* 155 (2006) 401–414.
- [3] Z. Chen, Y. Qin, K. Amine, *Electrochim. Acta* 54 (2009) 5605–5613.
- [4] W. Weng, Z. Zhang, P.C. Redfern, L.A. Curtiss, K. Amine, *J. Power Sources* 196 (2011) 1530–1536.
- [5] J. Wen, Y. Yu, C. Chen, *Mater. Express* 2 (2012) 197–212.
- [6] S. Abada, G. Marlair, A. Lecocq, M. Petit, V. Sauvant-Moynot, F. Huet, *J. Power Sources* 306 (2016) 178–192.
- [7] Q. Wang, P. Ping, X. Zhao, G. Chu, J. Sun, C. Chen, *J. Power Sources* 208 (2012) 210–224.
- [8] A.W. Golubkov, D. Fuchs, J. Wagner, H. Wiltsche, C. Stangl, G. Fauler, G. Voitic, A. Thaler, V. Hacker, *RSC Adv.* 4 (2014) 3633–3642.
- [9] S.S. Zhang, *J. Power Sources* 162 (2006) 1379–1394.
- [10] L. Zhang, Z. Zhang, K. Amine, *Lithium Ion Batteries - New Developments*, InTech, 2012.
- [11] J. Huang, N. Azimi, L. Cheng, L.A. Shkrob, Z. Xue, J. Zhang, N.L. Dietz Rago, L.A. Curtiss, K. Amine, Z. Zhang, L. Zhang, *J. Mater. Chem.* 3 (2015) 10710–10714.
- [12] L. Zhang, Z. Zhang, K. Amine, *ECS Transactions* 45 (2013) 57–66.
- [13] L. Zhang, Z. Zhang, K. Amine, I. Belharouak (Ed.), *Lithium Ion Batteries - New Developments*, InTech, 2012, <http://dx.doi.org/10.5772/13587>.
- [14] L. Zhang, Z. Zhang, P.C. Redfern, L.A. Curtiss, K. Amine, *Energy Environ. Sci.* 5 (2012) 8204–8207.
- [15] L. Zhang, J. Huang, K. Youssef, P.C. Redfern, L.A. Curtiss, K. Amine, Z. Zhang, *J. Electrochem. Soc.* 161 (2014) A2262–A2267.
- [16] M. Adachi, K. Tanaka, K. Sekai, *J. Electrochem. Soc.* 146 (1999) 1256–1261.
- [17] C. Buhmester, J. Chen, L. Moshurchak, J. Jiang, R.L. Wang, J.R. Dahn, *J. Electrochem. Soc.* 152 (2005) A2390–A2399.
- [18] J. Huang, B. Pan, W. Duan, X. Wei, R.S. Assary, L. Su, F.R. Brushett, L. Cheng, C. Liao, M.S. Ferrandon, W. Wang, Z. Zhang, A.K. Burrell, L.A. Curtiss, I.A. Shkrob, J.S. Moore, L. Zhang, *Sci. Rep.* 6 (2016) 32102.
- [19] R.L. Wang, J.R. Dahn, *J. Electrochem. Soc.* 153 (2006) A1922–A1928.
- [20] J. Zhang, Z. Yang, I.A. Shkrob, R.S. Assary, S. o. Tung, B. Silcox, W. Duan, J. Zhang, C.C. Su, B. Hu, B. Pan, C. Liao, Z. Zhang, W. Wang, L.A. Curtiss, L.T. Thompson, X. Wei, L. Zhang, *Adv. Energy Mater.* (2017) 1701272.
- [21] N. Membrèño, K. Park, J.B. Goodenough, K.J. Stevenson, *Chem. Mater.* 27 (2015) 3332–3340.
- [22] Z. Guo, Z. Chen, *J. Electroanal. Chem.* 754 (2015) 148–153.
- [23] D. Li, D.L. Danilov, L. Gao, Y. Yang, P.H.L. Notten, *Electrochim. Acta* 210 (2016) 445–455.
- [24] K. Amine, J. Liu, I. Belharouak, *Electrochem. Commun.* 7 (2005) 669–673.
- [25] S. Wang, P. Kuo, C. Hsieh, H. Teng, *ACS Applied Materials & Interfaces* 6 (2014) 19360–19370.
- [26] H. Wu, C. Su, D. Shieh, M. Yang, N. Wu, *Electrochem. Solid State Lett.* 9 (2006) A537–A541.
- [27] K. Xu, *Chem. Rev.* 114 (2014) 11503–11618.
- [28] I.A. Shkrob, Y. Zhu, T.W. Marin, D. Abraham, *J. Phys. Chem. C* 117 (2013) 19255–19269.
- [29] W. Huang, Y. Yan, C. Wan, C. Jiang, J. Ying, *Chin. J. Power Sci.* (2001) 91–93.